Microstrip Antenna Arrays for Implantable and Wearable Wireless Applications

Daniel G. Rucker[1], Haider R. Khaleel[1], Sunny S. Raheem[2], and Hussain M. Al-Rizzo[2]

[1] Department of Applied Science
[2] Department of Systems Engineering
University of Arkansas at Little Rock
2801 South University Ave., Little Rock, AR 72204, USA
{dxrucker,hrkhaleel,ssraheem,hmalrizzo}@ualr.edu

Abstract. Flexible microstrip antenna arrays have become a necessity in today's miniaturized biomedical wireless devices. Implantable and wearable biomedical devices such as pacemakers, drug delivery systems, heart rate monitors, and respiratory monitors need to communicate with exterior base station devices and relayed to healthcare professionals. In this paper, multiple flexible microstrip antenna arrays are designed and simulated for these applications. The frequency bands of 5.2 GHz and 5.8 GHz are utilized to provide a high bandwidth communication link. CST Microwave Studio was used for the modeling and simulation of the antennas. The reflection coefficient, gain, and correlation coefficient for each antenna are presented and discussed. The presented antennas can be utilized together as an array for enhanced gain or independently in a Multiple Input Multiple Output (MIMO) system.

Keywords: Implantable and Wearable Antenna, Microstrip Antenna Array, MIMO.

1 Introduction

Microstrip antenna arrays have enjoyed many uses in today's world of miniaturized wireless devices. The ever increasing demand for smaller and affordable devices with greater operating capabilities has increased the requirements for small microstrip antennas with high efficiencies, gains, and bandwidths [1,2]. In order to meet these needs, the next generation of miniaturized antenna arrays must be developed. Microstrip antennas that function as arrays for either enhanced gain or Multiple Input Multiple Output (MIMO) systems can provide next generation, high data rate wireless systems. For high data rate applications such as wireless local area networks (WLAN), the 5.2 GHz and 5.8 GHz bands are available. The 5.2 GHz band ranges from 5.15 GHz to 5.35 GHz and the 5.8 GHz band ranges from 5.725 GHz to 5.875 GHz.

Today's implantable biomedical systems require wireless links to provide feedback to healthcare professionals. Implantable devices such as pacemakers, drug delivery systems, and in-vivo electroencephalogram (EEG) can utilize wireless links to send data to collection units outside the body thus eliminating hard wire connections [3,4].

J. Lin and K.S. Nikita (Eds.): MobiHealth 2010, LNICST 55, pp. 135–143, 2011.

Wearable biomedical systems also benefit from wireless links. Applications such as heart rate and respiratory monitors have been used in patient care and sports medicine. By utilizing a wireless link for a wearable system, a runner could utilize a wearable system to provide data on heart rate and respiratory rate while tracking speed and position using a global positioning system (GPS) [5]. A recent growing trend is the integration of wireless connectivity with secure digital (SD) flash memory cards [6]. By using this form factor for the design, antennas and associated circuitry can be integrated with a device's memory all in one package.

Computer modeling and simulation tools provide researchers with the ability to design and fabricate antennas by avoiding the expensive trial and error approach. This allows for many designs to be studied and refined before fabricating the prototypes. CST Microwave Studio (MWS) is a modeling and simulation software package used for antennas and high frequency structures [7]. MWS uses the Finite Integration Technique for time domain simulations.

In this paper, a series of printed microstrip antenna arrays on thin substrates are designed and analyzed. The development of thin, printed arrays is presented as a progression from printed dipoles to square patches then to spiral patches. The simulated S-Parameters, gain, and correlation coefficient results are shown. The antenna arrays are intended for use in Secure Digital (SD) memory card sized, thin, flexible substrates with maximum rectangular dimensions of 32 mm in length by 24 mm in width. The arrays are designed to provide wireless communication links for miniaturized implantable and wearable biomedical devices. The 5.2 GHz and 5.8 GHz frequency bands were selected to reduce the size of the antennas and to serve high data rate applications.

2 Flexible Antenna Design

Flexible microstrip antennas impose multiple design constraints when used for implantable and medical devices. For the prototype antenna arrays in this paper, the two main performance goals are a 5 dB gain and a correlation coefficient of less than 0.2. The arrays must be broadside radiating and nearly omnidirectional with respect to azimuth. The correlation coefficient can be calculated either from the three-dimensional far field radiation pattern (equation 1) which requires extensive calculations or from S-parameters (equation 2). However, in this study, the simulated correlation coefficient has been extracted from the far field analysis which is more accurate than the S-parameter method [8].

$$\rho = \frac{\iint_{4\pi} \bar{G}_1 \, \bar{G}_2{}^* \, d\Omega}{\sqrt{\iint_{4\pi} \bar{G}_1 \, \bar{G}_1{}^* d\Omega \iint_{4\pi} \bar{G}_2 \, \bar{G}_2{}^* d\Omega}}. \tag{1}$$

$$\rho = \frac{|S_{11}{}^* S_{12} + S_{21}{}^* S_{22}|^2}{(1-(|S_{11}|^2+|S_{21}|^2))(1-(|S_{22}|^2+|S_{12}|^2))}. \tag{2}$$

For two uncorrelated antennas and a reasonable bit error rate, the diversity gain is equal to 10 dB (equation 3).

$$G = 10.\sqrt{1-|\rho|^2}. \tag{3}$$

2.1 Flexible Printed Dipole Antennas

The printed dipole design was chosen as the initial antenna design for this work. Printed dipoles have been reported in [9,10], among others, and will serve as a basis to compare against other designs. The center frequency of 5.8 GHz will serve high data rate applications while reducing the size compared to 2.45 GHz antennas. Two printed dipoles were modeled on a 100 μm polyamide substrate, with relative permittivity (ε_r) = 3.5, to investigate the use of thin printed dipoles on flexible substrates. The two dipoles were placed on a substrate with a length of 32 mm and width of 24 mm. The dimensions were taken from measurements of a SD memory card commonly used in cameras and other small personal devices. Fig. 1 shows the dipoles located on the thin substrate.

A perfect electric conductor (PEC) is used as the material for the dipole arms to limit the mesh size. The mesh is limited because MWS does not mesh PEC, therefore avoiding a very fine mesh gradient. The substrate does use the MWS default loss tangent of 0.003 for the polyamide. The antenna from Fig. 1 was further developed by adding a microstrip line to feed both antennas. Fig. 2 shows the antenna with the added microstrip line feed. The substrate has been rendered colorless in order to better display both the feed and ground strip. The independently fed dipole antennas required a feed with an input impedance of 72 Ω for correct input matching. The single microstrip line fed dipoles were designed to match to a 50 Ω microstrip line. This allows for the antenna to operate with a standard input impedance common to RF transceiver board SMA connectors.

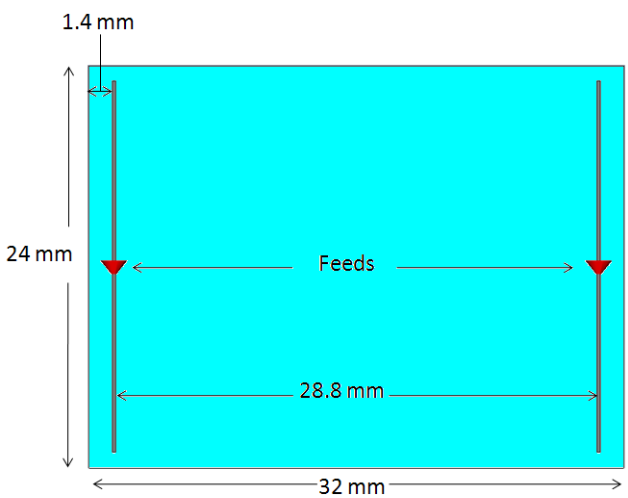

Fig. 1. Printed Dipole Antennas with Independent Feeds

The antenna was simulated using individual feeds and a common microstrip line feed to provide a comparison of the feeding techniques. The S_{11} results compare favorably well within the 5.8 GHz band as seen in Fig. 3. Both antennas share a -10 dB bandwidth of 562 MHz ranging from 5.447 GHz to 6.009 GHz. The far-field gain

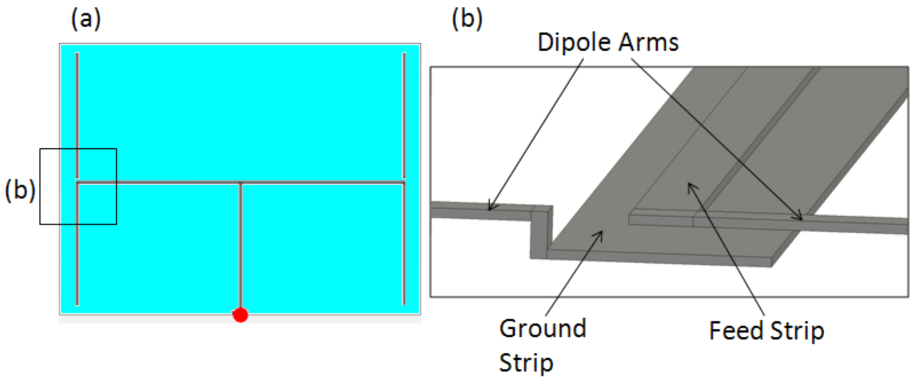

Fig. 2. Printed Dipole Antennas with a Single Feed

pattern of both antennas compares very closely at 5.8 GHz in magnitude and shape. The bore-sight gains of the independent fed and single fed dipoles are 6.6 dB and 6.5 dB, respectively, and both have a half-power beamwidth of 78°. The E-plane and H-plane polar cuts for the single fed dipoles are shown in Fig. 4. Since both dipole gain patterns are approximately equal, Fig. 4 is representative of both arrays. The correlation coefficient calculated from the three dimensional radiation pattern is 0.013. This would allow for the independently fed dipoles to be used for MIMO applications.

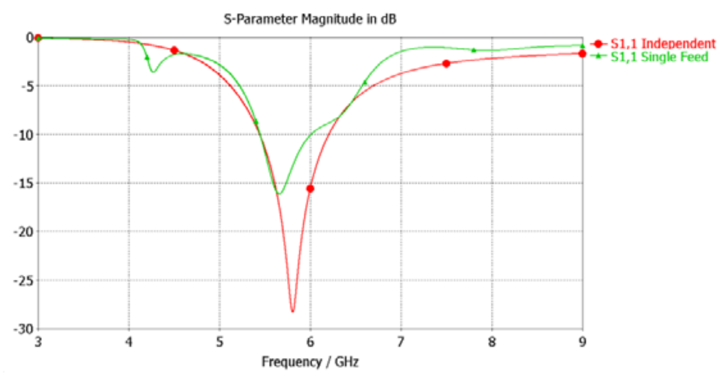

Fig. 3. Printed Parallel Dipole Array S_{11}, Single and Two Feeds

2.2 Flexible Printed Square Patch Antennas

The flexible printed square patch antenna design used in this work consists of a microstrip line feed and square inset patch geometry. The basic patch design for the printed square antenna with an inset fed microstrip line is shown in Fig. 5. W, L, W_f, Y_0 are the four parameters needed to design this patch to operate in the desired resonate frequency of 5.8 GHz. W is the patch width and L is the patch length. W_f is width of the microstrip feed line and also the inset gap width between the feed line and the patch. Y_0 is the adjustable inset length to change the matching impedance of the microstrip line to the patch edge [11].

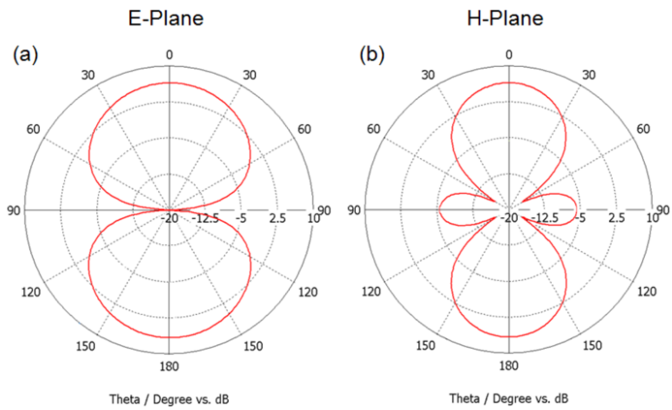

Fig. 4. Parallel Dipole Array, Independent Feeds, Gain E-plane (a) and H-plane (b)

The same flexible polyamide substrate (ε_r = 3.5) as the dipole antennas is used in the design of this square microstrip line fed antenna array. Since this patch is fed through a microstrip line, the width of the microstrip line (W_f) must be calculated in order to match the input impendence. In this design, the input impendence is 50 Ω, thus requiring the width of the microstrip line to be 0.2278 mm. The adjustable inset distance (Y_0) was adjusted to 1.25 mm long resulting in better matching for this antenna to operate at the needed frequency. A parametric sweep was used to determine the appropriate length of the inset. The width of this antenna is 12.00 mm, while the length is 13.752 mm. The distance between the two patches is 6mm (0.217λ). The patch design with dimensions is displayed in Fig. 5. The patch length is adjusted in order to ensure a center frequency of 5.797 GHz with a reflection coefficient of -16 dB, which is displayed in S parameter Fig. 6. The correlation coefficient of 0.204 was calculated from the three dimensional far-field results. Fig. 7 displays the E-Plane and the H-Plane two dimensional graphs of the far-field gain pattern. The main lobe shows the expected radiation pattern of a broadside radiator and has gain 5.3 dB. The angular width (3dB) is 88.5 degrees.

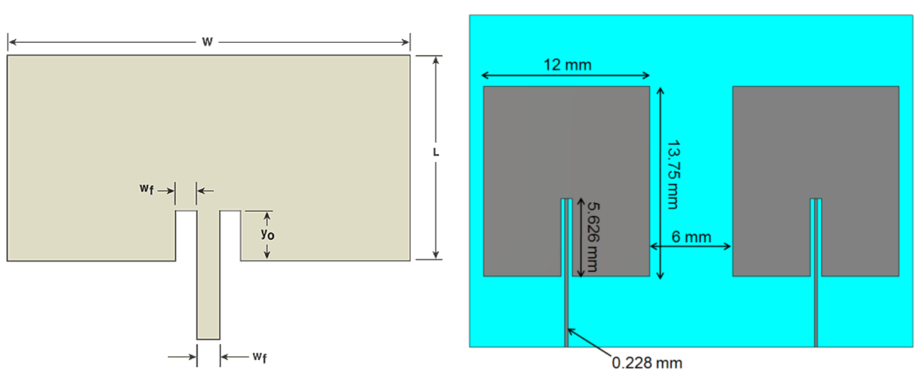

Fig. 5. Square Inset Fed Patch Geometry and Square Microstrip Antenna Array

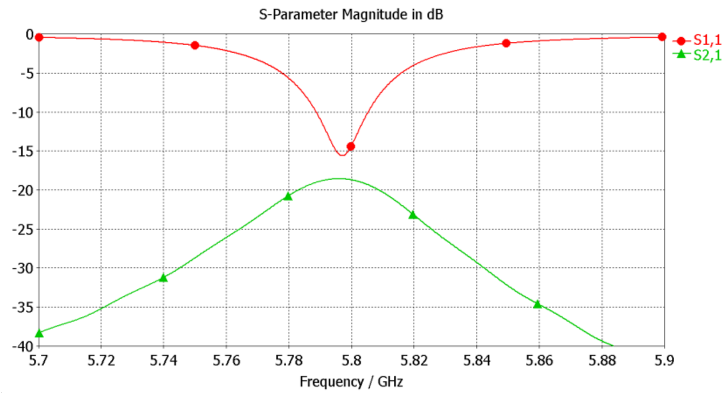

Fig. 6. S-Parameter Results of Double Square Microstrip Fed Patch Antenna

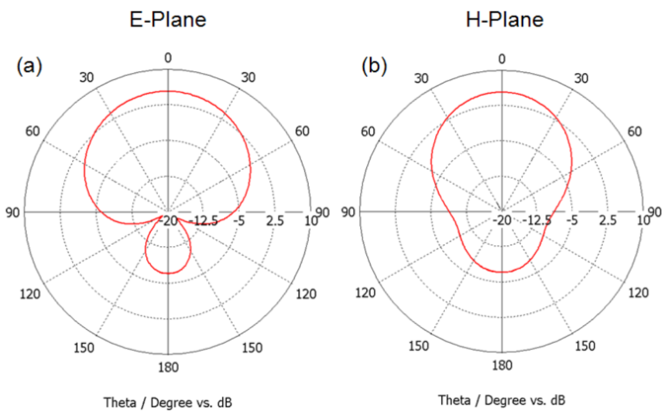

Fig. 7. Square Microstrip Antenna Array

2.3 Flexible Printed Spiral Antennas

The printed spiral antennas were designed to utilize the same SD card form factor size as used on the two previous designs. Two 10 mm × 10 mm rectangular spiral antennas with a 0.7 mm strip width and a 0.5 mm gap was placed on a 22 mm × 30 mm substrate backed by a ground plane. The spiral was designed to resonate at 5.2 GHz which is suitable for WLAN applications. In an attempt to reduce the mutual coupling between the radiating elements, a spiral slit is utilized to produce a defect in the ground plane.

The proposed slit structure consists of a 3-turn spiral with a strip width of 0.4 mm and a 0.5 mm gap except in the center which has a 1.5 mm gap. The structure is positioned at the middle of the ground plane. The front and back views of the antenna model are presented in Fig. 8. The thickness of the substrate is 0.85 mm with a relative permittivity of 5.25 while the inter-element distance is 9 mm (0.36λ). A parametric study was performed for the two coaxial feed locations to achieve optimal impedance matching.

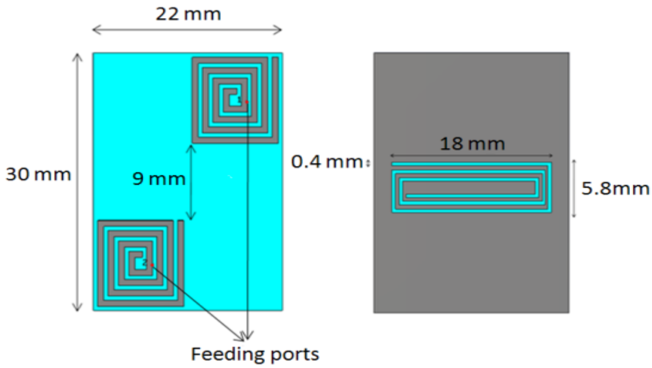

Fig. 8. Microstrip Spiral Antenna Array, Front View (left) and Back View (right)

The simulated *S*-parameters for the proposed design with and without a ground plane slit are provided in Fig. 9. From the S_{11} results, a return loss of -35 dB at 5.2 GHz is observed for the design without spiral slit. A slight shift in the resonance frequency with a spiral slit is noticed with a return loss of -30 dB. This shift can be compensated for by adjusting the patch length in order to keep the patch resonance frequency identical in both cases. The simulated -10 dB bandwidth is 20 MHz. The mutual coupling between the two spiral elements was analyzed based on transmission coefficient (S_{21}) between the two feeding ports. Obviously, the design with the spiral slit provides further isolation between the radiating elements compared to the conventional design with the same element separation. This behavior can be explained as follows: A portion of surface current is trapped by the spiral ground plane slit between the radiating patch elements which lead to reduced current coupling. This shows that the flow of current from one edge of the ground plane to the other edge is decreased which helps to reduce the mutual coupling between the two radiating elements [12]. Due to this effect, a reduction of 3.3 dB in mutual coupling is achieved.

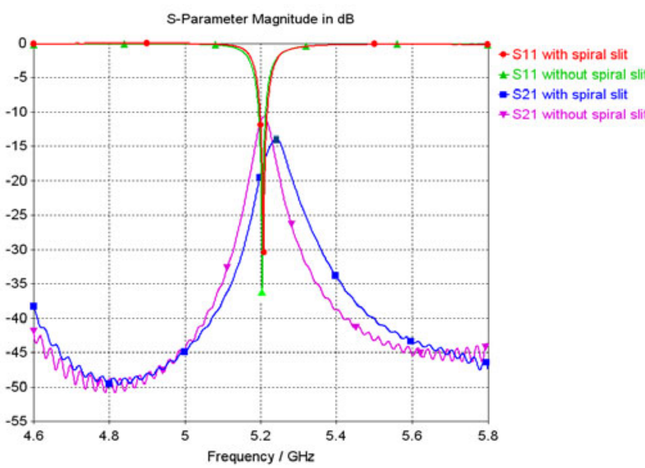

Fig. 9. Simulated S-Parameter for the proposed design with and without spiral ground plane slit

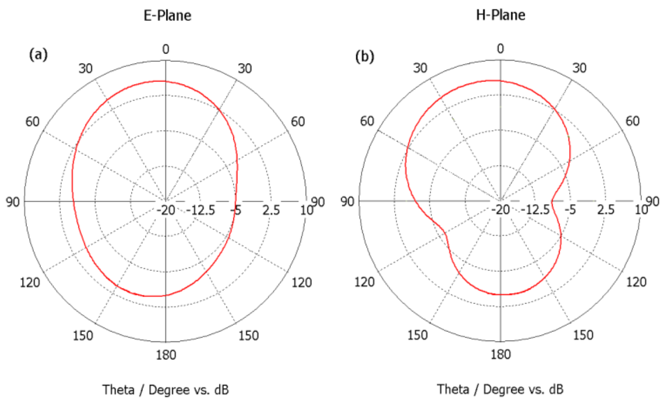

Fig. 10. Microstrip Spiral Array with ground plane slit, Gain E-plane (a) and H-plane (b)

The simulated correlation coefficient is 0.2, along with a diversity gain of 9.8 dB and a 5.7 dB combined elements gain at 5.2 GHz comply with the WLAN technology design requirements. The simulated E-plane and H-plane far field radiation patterns in the presence of the spiral ground plane slit are presented in Fig. 10.

3 Conclusion

In this paper, we presented three antenna arrays to achieve our design goals of SD memory card size, far-field gain, and correlation coefficient for the application of wireless biomedical devices. The printed dipole antenna array provide an effective implementation of a popular design. The microstrip square patch antenna array provides a popular design for comparison. Then, the square spiral microstrip antenna array was designed to achieve a lower resonant frequency while maintaining the same form factor of the dipole and square patch arrays. The results show the spiral array achieved a similar far-field gain pattern to the printed dipoles and square patches while providing a lower resonant frequency of 5.2 GHz. The printed dipole array achieved the highest bandwidth at 562 MHz. The printed dipole array and the spiral array both have merit for implantable and wearable biomedical wireless devices. These antennas will assist 21st century medical professionals to provide better healthcare while being less evasive to the hospital patient or the sports athlete.

Acknowledgement. This research was funded in part by the National Science Foundation Grant EPS-0701890.

References

1. Park, S., Jayaraman, S.: Enhancing the Quality of Life Through Wearable Technology. In: IEEE Engineering in Medicine and Biology Magazine. pp. 41–48 (May/June 2003)
2. Rahmat-Samii, Y.: Wearable and Implantable Antennas in Body-Centric Communications. In: The 2nd European Conference on Antennas and Propagation, pp. 1–5 (November 2007)

3. Soontornpipit, P., Furse, C.M., Chung, Y.C.: Design of Implantable Microstrip Antenna for Communication with Medical Implants. IEEE Transactions on Microwave Theory and Techniques 52(8), 1944–1951 (2004)
4. Rucker, D., Al-Alawi, A., Adada, R., Al-Rizzo, H.M.: A Miniaturized Tunable Microstrip Antenna for Wireless Communications with Implanted Medical Devices. In: Proceedings of the 2nd International Conference on Body Area Networks Conference, Florence, Italy (June 2007)
5. Jovanov, E., Milenkovic, A., Otto, C., de Groen, P.: A wireless body area network of intelligent motion sensors for computer assisted physical rehabilitation. Journal of Neuro Engineering and Rehabilitation 2(6) (March 2005)
6. Eye-Fi SD Memory Cards with WiFi (April 2010), `http://www.eye.fi/products/connectx2`
7. CST Microwave Studio (April 2010), `http://www.cst.com/Content/Products/MWS/Overview.aspx`
8. Blanch, S., Romeu, J., Corbella, I.: Exact representation of antenna system diversity performance from input parameter description. Electronic Letters 39, 705–707 (2003)
9. Pozar, D.M.: Analysis of Finite Phased Arrays of Printed Dipoles. IEEE Transactions on Antennas and Propagation 33(10), 1045–1053 (1985)
10. Duffley, B.G., Morin, G.A., Mikavica, M., Antar, Y.M.M.: A Wide-Band Printed Double-Sided Dipole Array. IEEE Transactions on Antennas and Propagation 52(2), 628–631 (2004)
11. Ramesh, M., Yip, K.B.: Design Formula for Inset Fed Microsrtip Patch Antenna. Journal of Microwaves and Optoelectronics 3(3) (December 2003)
12. Chiu, C., Cheng, C., Murch, R.D., Rowell, C.R.: Reduction of Mutual Coupling Between Closely-Packed Antenna Elements. IEEE Transactions on Antennas Propagation 55(6), 1732–1738 (2007)